Pergamon

Tetrahedron 57 (2001) 9799–9812

TETRAHEDRON

Conformational analysis of highly hindered thiophosphoramidates

Zaira J. Domínguez,[†] M[a] Teresa Cortez and Barbara Gordillo[*]

Departamento de Química, Centro de Investigación y de Estudios Avanzados del Instituto Politécnico Nacional, Apartado Postal 14-740, Mexico, DF, Mexico

Received 21 August 2001; accepted 3 October 2001

Abstract—The conformational analyses in solution and in solid state of the highly crowded mobile systems, 2-dicyclohexylamino-2-thio-1,3,2λ^5-dioxaphosphinane (**1**), 2-dicyclohexylamino-2-thio-*trans*-4,6-dimethyl-1,3,2λ^5-dioxaphosphinane (*trans*-**2**) and their anancomeric analogs, *ax*-2-dicyclohexylamino-2-thio-*cis*-4,6-dimethyl-1,3,2λ^5-dioxaphosphinane (*ax-cis*-**2**) and *eq*-2-dicyclohexylamino-2-thio-*cis*-4,6-dimethyl-1,3,2λ^5-dioxaphosphinane (*eq-cis*-**2**) are informed. In accordance with proton–proton and proton–phosphorus coupling constants, the dioxaphosphinane ring adopts a chair conformation in all compounds except in the case of *trans*-**2**, which was found in a twisted conformation. Solid state structural analyses suggest that only the synaxial Me/NR$_2$ or Me/S interactions in *trans*-**2**, force the heterocycle ring to remain as a mixture of twisted boat and half-chair (chaise loungue) conformers. © 2001 Elsevier Science Ltd. All rights reserved.

1. Introduction

Thiophosphoramidates are phosphorus thioesters that resembles, phosphoramidites (Scheme 1a) used by Letsinger–Caruthers[1] in the oligonucleotide synthesis of the DNA chain. The biochemical activity of phosphorus containing biomolecules depends largely on conformation, an example is found in the interaction of *c*AMP (Scheme 1b)–protein, in the cytoplasm of the liver cell. This interaction gives rise to the production of the enzyme that catalyzes the glycogenolysis process for the production of glucose in the organism.[2]

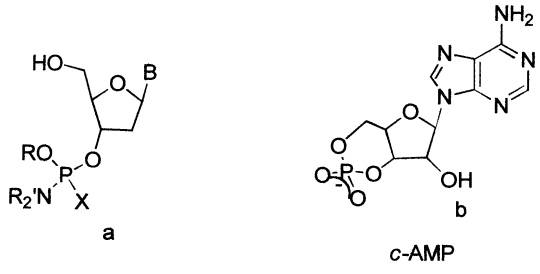

B = adenine, guanine, thymine;
R, R' = alkyl or aryl group
X = lone pair (phosphoramidite)
X = O (phosphoramidate)
X = S (thiophosphoramidate)

Scheme 1.

Six-membered ring phosphorus containing heterocycles are very flexible systems, they often adopt twist conformations[3–9] in addition to the chair, which is commonly found in cyclohexanes and 1,3-dioxanes. For example, Bentrude and Yee[9] reported that the *cis*-2,5-di-*tert*-butyl-2-oxo-1,3,2λ^5-dioxaphosphinane (Scheme 2), is in solution in a conformational equilibrium chair–boat, being the boat conformation more populated than the chair ($\Delta G^0 = -0.8$ kcal/mol). The ΔG^0 for the chair–boat equilibrium was estimated to be around 1 kcal/mol, an extremely low value taking into consideration that a similar interconversion in cyclohexanes or 1,3-dioxanes is in between 3 and 8 kcal/mol.[10,11]

In addition, it is well known[3,7,8,12] that the conformational preference of the substituents at the phosphorus atom are, in a great extent, related to their electronic nature. Thus, when the substituent is an electron withdrawing atom or group (i.e. Cl, OMe), it prefers to occupy the axial position; this behavior has been attributed to the attractive

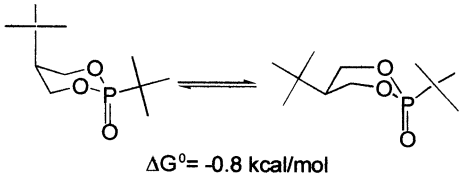

Scheme 2.

Keywords: dioxaphosphinanes; conformation; NMR; X-ray crystal structures.

* Corresponding author. Tel.: +525-5747-3729; fax: +525-5747-7113; e-mail: ggordill@mail.cinvestav.mx

† Department of Chemistry and Biochemistry, University of California, Los Angeles, CA, USA.

0040–4020/01/$ - see front matter © 2001 Elsevier Science Ltd. All rights reserved.
PII: S0040-4020(01)00997-8

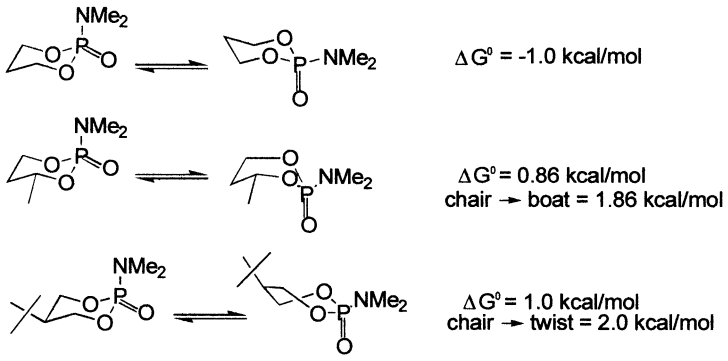

Scheme 3.

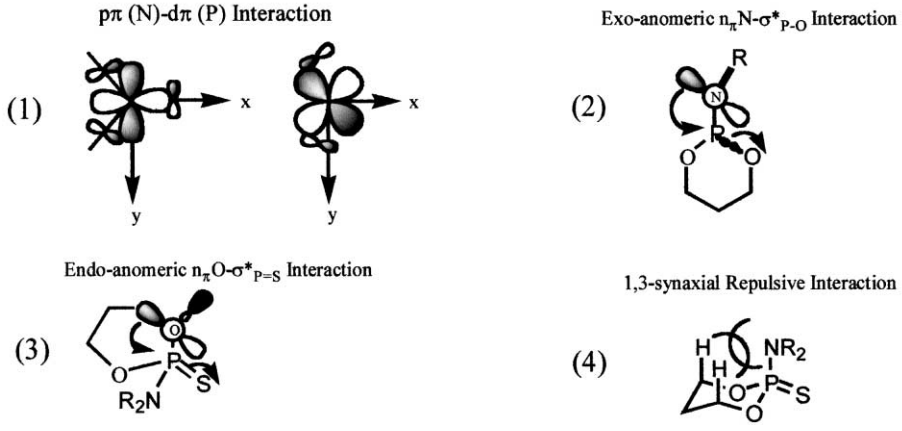

Scheme 4.

stereoelectronic interaction $n_{\pi}O-\sigma^{*}_{P\text{-substituent}}$, which takes place only in the axial isomer. Contrarily, when the substituent is an amino group (NR_2 with R=H or alkyl) the preference for the equatorial orientation overcome the axial[7,8,13,14] so that for example the equilibrium of the 2-dimethylamino-2-oxo-1,3,2λ^5-dioxaphosphinane of Scheme 3, is shifted toward the equatorial isomer for 1.0 kcal/mol.

The equatorial preference of the NR_2 group has been ascribed to various causes (Scheme 4): (1) the maximal pπ(N)–dπ(P) interaction between the nitrogen lone pair localized in a p orbital and one of the empty d orbitals of phosphorus,[15] (2) the stabilizing $n_{\pi}N-\sigma^{*}_{P-O}$ *exo*-anomeric interaction,[3,16] (3) the stabilizing $n_{\pi}O-\sigma^{*}_{P=S}$ *endo*-anomeric interaction,[17] and/or (4) the repulsive 1,3-synaxial interaction between the R groups bonded to the nitrogen atom and the axial hydrogens at 4 and 6 position of the dioxaphosphinane ring.[7] Although it is worth of mention, that theoretical studies performed recently on phosphorus compounds[18,19] have provided evidence against the participation of d orbitals of phosphorus in their stabilization, even in molecules with low-lying acceptor orbitals such as those that contain PO and PS groups. Based on these arguments, we assume that the *exo*-anomeric $n_{\pi}N-\sigma^{*}_{P-O}$ stabilization, the *endo*-anomeric $n_{\pi}O-\sigma^{*}_{P=S}$ stabilization and/or the repulsive 1,3-synaxial interaction mentioned earlier are more important to rationalize the equatorial preference of the amino group in the 1,3,2λ^5-dioxaphosphinanes studied here.

Reported in this work, are the conformational analyses of mobile, and anancomeric highly hindered thiophosphoramidates, 2-dicyclohexylamino-2-thio-1,3,2λ^5-dioxaphosphinane (**1**), 2-dicyclohexylamino-2-thio-*trans*-4,6-dimethyl-1,3,2λ^5-dioxaphosphinane (*trans*-**2**), *ax*-2-dicyclohexylamino-2-thio-*cis*-4,6-dimethyl-1,3,2λ^5-dioxaphosphinane (*ax-cis*-**2**), and *eq*-2-dicyclohexylamino-2-thio-*cis*-4,6-dimethyl-1,3,2λ^5-dioxaphosphinane (*eq-cis*-**2**) of Scheme 5. Stereoelectronic and steric interactions are analyzed in light of the conformational analysis in solution by NMR and the structural parameters of the X-ray structures.

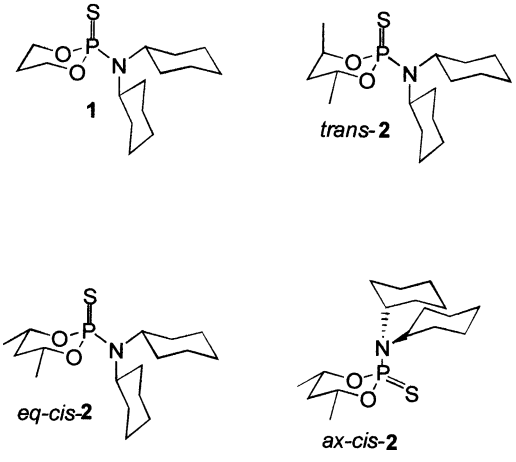

Scheme 5.

2. Results

The synthesis of **1** and the configurational isomers of **2** was accomplished as summarized in Scheme 6. Products were purified by column chromatography. Due to the fact that the compounds display strong steric interactions, they were not formed extensively; hence, isolated yields are modest.

The spectra were obtained at 27°C, using $CDCl_3$ as solvent; the complete assignment of proton (Table 1) and carbon-13 signals (Table 2), was achieved by means of ^1H, ^1H and ^1H, ^{13}C correlated 2D NMR spectra, as well as inverse ^1H detected HMQC and HMBC experiments. Selected backbone coupling constants in proton NMR were obtained through homonuclear decoupling experiments (Table 3). The four compounds presented in this work were solids; after recrystallization they afforded crystals suitable for X-ray diffraction analysis allowing their conformational studies in solid state to be performed.

3. Discussion

NMR analysis. As observed in Table 3, the vicinal $^3J_{H4aH5a}$ for the compounds **1**, *ax-cis*-**2** and *eq-cis*-**2** of around 12 Hz (*anti* arrangement), and $^3J_{H4aH5e}$ in between 2.2 and 4.5 Hz (*gauche* arrangement) suggest that these molecules are in solution in a chair conformation. Besides, the $^3J_{H4(6)aP}$ and the $^4J_{H7(8)P}$ coupling constant in the anancomeric *ax-cis*-**2** and *eq-cis*-**2** with values of 2.2 and 1.5–1.6 Hz for both compounds, are also in agreement with a chair conformation.[3,7] In the mobile system **1**, the remarkable difference between $^3J_{H4(6)aP}$ and $^3J_{H4(6)eP}$ coupling constants (2.4 and 25.3 Hz, respectively), led us to conclude that in the equilibrium, this molecule is also highly biased toward one chair conformation.[8,20] Moreover, for compound **1** was observed a splitting of the H_{4e} signal (δ 4.2 ppm) of 2.3 Hz which correspond to a cross-ring Heq–Heq coupling. This cross-ring coupling has been observed for analogous compounds in chair conformations.[21–23] In ^{13}C NMR, the $^3J_{CP}$ coupling constants of the methyl groups at positions C_7 and C_8 for *eq-cis*-**2** and *ax-cis*-**2** (9.9 and 7.7 Hz, respectively), are also indicative of locked chair conformations, whereas for *trans*-**2**, there is a difference between $^3J_{CP}$ of the corresponding methyl groups of 6.9 Hz.

Conformational equilibria. Once the NMR parameters, like chemical shifts and coupling constants, of the mobile thiophosphoramidate **1** and *trans*-**2** and the anancomeric *eq-cis*-**2** and *ax-cis*-**2** have been determined, it is possible, in principle, to evaluate the conformational equilibria shown in Scheme 7 by using Eliel's equation (Eq. (1)),[24] where X_A

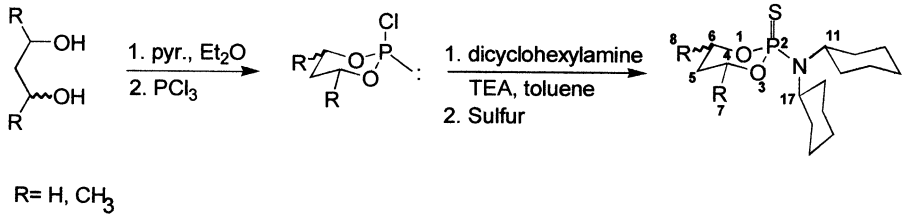

Scheme 6.

Table 1. ^1H NMR chemical shifts (ppm) for thiophosphoramidates **1** and **2** in $CDCl_3$

Chemical shifts (δ)	Compound			
	1	*eq-cis*-**2**	*ax-cis*-**2**	*trans*-**2**
H4a	4.71	4.79	4.47	4.9
H4e	4.20	–	–	–
H5a	2.20	1.53	2.01	1.89
H5e	1.55	1.69	1.69	1.93
H6a	4.71	4.79	4.47	–
H6e	4.20	–	–	4.61
H7	–	1.31	1.39	1.35
H8	–	1.31	1.39	1.60
Hcyclohex.	3.41 (2H)	3.46 (2H)	3.17 (2H)	3.36 (2H)
	1.58–1.70 (14H)	1.60–1.85 (14H)	1.57–1.95 (14H)	1.53–1.85 (14H)
	1.09–1.30 (6H)	1.07–1.30 (6H)	1.08–1.28 (6H)	1.05–1.31 (6H)

Table 2. ^{13}C NMR signal assignments in thiophosphoramidates

Compound	C-4	C-5	C-6	C-7	C-8	C-11	C-12	C-13	C-14
1	66.6 (6.1)	26.7 (6.6)	66.6 (6.1)	–	–	57.4 (5.4)	33.5 (1.4)	27.0	25.8
eq-cis-**2**	72.7 (5.4)	41.3 (3.8)	72.7 (5.4)	22.4 (9.9)	22.4 (9.9)	57.1 (4.6)	33.2	26.7	25.6
ax-cis-**2**	75.0 (8.5)	39.8 (7.7)	75.0 (8.5)	22.4 (7.7)	22.4 (7.7)	57.0 (3.8)	33.3 (3.1)	26.8	25.7
trans-**2**	69.4 (5.4)	37.8 (7.7)	74.5 (6.9)	22.4 (9.2)	21.9 (2.3)	57.1 (5.4)	33.2 (3.1)	26.8	25.6

Chemical shifts (δ) in ppm from TMS in $CDCl_3$. In parentheses J_{CP} in Hz.

Table 3. ^{1}H NMR backbone coupling constants (Hz) for Thiophosphoramidates **1**, and **2**. First-order analysis in $CDCl_3$ at 27°C

Coupling constants	**1**	*eq-cis*-**2**	*ax-cis*-**2**	*trans*-**2**
$^{3}J_{H4aH5a}$	12.9	11.7	11.5	7.0
$^{3}J_{H4aH5e}$	4.5	2.2	2.2	5.2
$^{3}J_{H6aH5a}$	12.9	11.7	11.5	–
$^{3}J_{H6aH5e}$	4.5	2.2	2.2	–
$^{3}J_{H6eH5a}$	4.9	–	–	4.7
$^{3}J_{H6eH5e}$	2.3	–	–	4.7
$^{3}J_{H4aH7}$	–	6.1	6.3	6.9
$^{3}J_{H4eH7}$	–	–	–	–
$^{3}J_{H6aH8}$	–	6.1	6.3	–
$^{3}J_{H6eH8}$	–	–	–	6.2
$^{2}J_{H5aH5e}$	14.4	13.9	14.3	14.2
$^{2}J_{H4aH4e}$	10.3	–	–	–
$^{2}J_{H6aH6e}$	10.3	–	–	–
$^{3}J_{H4aP}$	2.4	2.2	2.2	3.5
$^{3}J_{H4eP}$	25.3	–	–	–
$^{4}J_{H5aP}$	–	–	–	1.2
$^{4}J_{H5eP}$	Overlapped signals	2.2	2.2	Overlapped signals
$^{3}J_{H6eP}$	25.3	–	–	15.6
$^{3}J_{H6aP}$	2.4	2.2	2.2	–
$^{4}J_{H7P}$	–	1.6	1.5	1.7
$^{4}J_{H8P}$	–	1.6	1.5	–
$^{3}J_{H11P}$	20.1	19.9	17.4	19.9
$^{3}J_{H17P}$	20.1	19.9	17.4	19.9

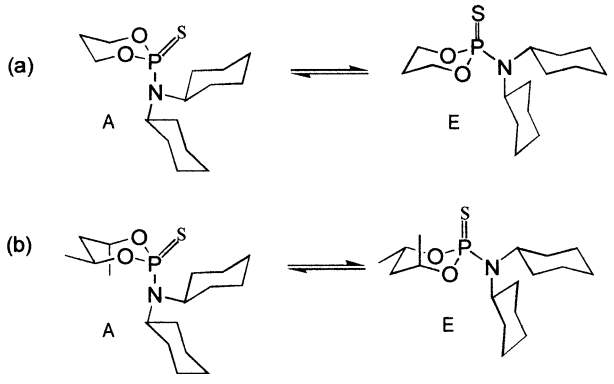

Scheme 7.

correspond to the magnetic property (δ and/or J) for the anancomeric *ax-cis*-**2** isomer, X_E for the *eq-cis*-**2**, and X to the mobile system **1** (Scheme 7a) or *trans*-**2** (Scheme 7b).

$$K = (X_A - X)/(X - X_E) \quad (1)$$

It is evident that Eq. (1) can only be applied when the value of the chemical shift or coupling constant for the mobile system is in between the corresponding for the two anancomeric axial and equatorial compounds; in other words, NMR parameters are averaged over the two conformations.[25] In order to calculate K for the equilibrium of compound **1**, two NMR parameters were taken into account, the chemical shift δ_{H4a} and the coupling constant $^{2}J_{C4(6)P}$, which independently gave values of K=(4.47 ppm−4.71 ppm)/(4.71 ppm−4.79 ppm)=3.0; and K=(8.5 Hz−6.1 Hz)/(6.1 Hz−5.4 Hz)=3.43 and an average ΔG^0 (25°C) of −0.69 kcal/mol in favor of the equatorial conformer. However, somewhat at odds, calculation of K with $^{3}J_{C5P}$ gave a value of 0.39, consequently a ΔG^0 (25°C) of 0.55 kcal/mol favoring the axial isomer. We believe that this calculation is not correct since it is not reflecting the equatorial preference of the $N(C_6H_{11})_2$ group found in solid state (as discussed later). An explanation of this result is the one given by McKenna;[25] however, in our opinion, distortion of the ring in the anancomeric models can be discarded based on the similarities between the structural parameters of mobile **1** and anancomeric *eq-cis*-**2** found by X-ray crystallography (Tables 5–7). Alternatively, a likely explanation for this unexpected result, is that the equilibrium is highly shifted toward the equatorial chair conformation, therefore calculation of K with equation **1** has led to inaccurate values. In fact by performing the calculation of the mole fraction (N) of the major conformer as suggested by Katritzky[23] and Edmundson[26] (Eqs. (2) and/or (3)), we could support this hypothesis

$$J_{POCH'} = J_t(N) + J_g(1 - N) \quad (2)$$

$$J_{POCH''} = J_g(N) + J_t(1 - N) \quad (3)$$

Where J_t and J_g are the vicinal coupling constants *trans* and *gauche*, respectively, of the acyclic homolog. These coupling constants are related to the average coupling constant of the acyclic system through Eq. (4)

$$J_t(1/3) + J_g(2/3) = J_{POCH}(acyc) \quad (4)$$

Based on the data reported by Katritzky et al.,[27] we decided to use a value of 10 Hz for J_{POCH}(acyc). Thus, by applying Eqs. (5) and (6) to calculate J_t and J_g, respectively [taking $J_{POCH'}$=$J_{H4(6)eP}$, and $J_{POCH''}$=$J_{H4(6)aP}$; then ($J_{POCH'}$+$J_{POCH''}$)=(25.3 Hz+2.4 Hz)=27.7 Hz for compound **1** in Table 3], we obtained J_t=25.4 Hz and J_g=2.3 Hz

$$J_t = 2(J_{POCH'} + J_{POCH''}) - 3J_{POCH}(acyc) \quad (5)$$

$$J_g = 3J_{POCH}(acyc) - (J_{POCH'} + J_{POCH''}) \quad (6)$$

Finally, substituting the values of J_t and J_g in Eq. (2) or Eq. (3), we were able to obtain N=0.996. This means that compound **1** is indeed locked in the major chair conformation with the amino group in the equatorial position. In consort, the ^{31}P chemical shift of compound **1** (72.7 ppm)

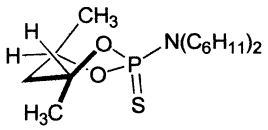

Figure 1.

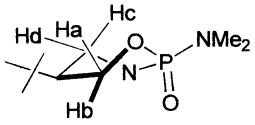

Figure 2.

is very close to the one of *eq-cis*-**2** (71.9 ppm), and apart from the *ax-cis*-**2** (67.0 ppm). Moreover, $^{3}J_{H4(6)aH5a}$ of 12.9 Hz and $^{3}J_{H4(6)aH5e}$ of 4.5 Hz or $^{3}J_{H4(6)eH5a}$ of 4.9 Hz also suggest a locked chair conformation for compound **1**.[8b] It is noteworthy that this result is *in-line* with ΔG^{0} values reported in the literature for amino groups in 1,3,2λ^{5}-dioxaphosphinanes; for example the equatorial preference of the dimethylamine group (a less steric demanding group than the dicycloamino group of compound **1**) in an analog phosphoramidate[28] is −1.1 kcal/mol, and almost the same value was found in the chair–chair equilibrium of the 5,5-dimethyl-2-oxo-2-di-*iso*propyl-amino-1,3,2λ^{5}-oxazaphosphinane reported by Bentrude et al.[29]

On the other hand, in the crowded *trans*-**2** isomer, we were also able to use two chemical shifts (δ_{H5a}, and δ_{C6}) and two coupling constant ($^{2}J_{C6P}$, and $^{3}J_{C7P}$) for the evaluation of K of the equilibrium shown in Scheme 7b through Eq. (1). The values found for K by using chemical shifts were 0.33 and 0.28, respectively, which correspond to an average ΔG^{0} (25°C)=0.71 kcal/mol favoring the axial isomer. Strikingly, the value of K calculated with the coupling constants was not consistent with the one calculated with chemical shifts, giving values of K=1.07 (with $^{2}J_{C6P}$) and K=2.14 (with $^{3}J_{C7P}$), thereby favoring the equatorial isomer. This inconsistence in the data was also observed when the percentage of the major isomer was calculated with Eqs. (2)–(6), therefore we thought of the possibility of using another expression of Eliel's equation[24] to calculate the mole fractions of every conformer in *trans*-**2** (Eq. (7))

$$J_{obs} = J_{conf}(A)(N_A) + J_{conf}(E)(N_E) \quad (7)$$

where, J_{obs} is the experimental coupling constant, $J_{conf}(A)$ and $J_{conf}(E)$ are the coupling constants of each independent conformer A and E in the equilibrium of *trans*-**2** (Scheme 7b), and N_A and N_E are the corresponding mole fractions. Since in the equilibrium, the coupling constants $^{3}J_{H6eH5e}$ and $^{3}J_{H4aH5e}$ of conformer (A) will become $^{3}J_{H6aH5a}$ and $^{3}J_{H4eH5a}$ of conformer (E) and substituting the values of the coupling constants of compound **1**, a conformationally locked system (mentioned earlier) [$^{3}J_{H4(6)aH5a}$=12.9 Hz, and $^{3}J_{H4(6)eH5e}$= 2.3 Hz, $^{3}J_{H4(6)eH5a}$=4.9 Hz and $^{3}J_{H4(6)aH5e}$=4.5 Hz] in Eq. (7), we could calculate the mole fractions N_A and N_E of *trans*-**2** as 56 and 44%, respectively, for the experimental J_{obs}(*trans*-**2**)=$^{3}J_{H4aH5a}$=7.0 Hz. On the other hand, when the calculation was performed with J_{obs}(*trans*-**2**)=$^{3}J_{H6eH5a}$=4.7 Hz, N_A, and N_E were 50 and 50%,

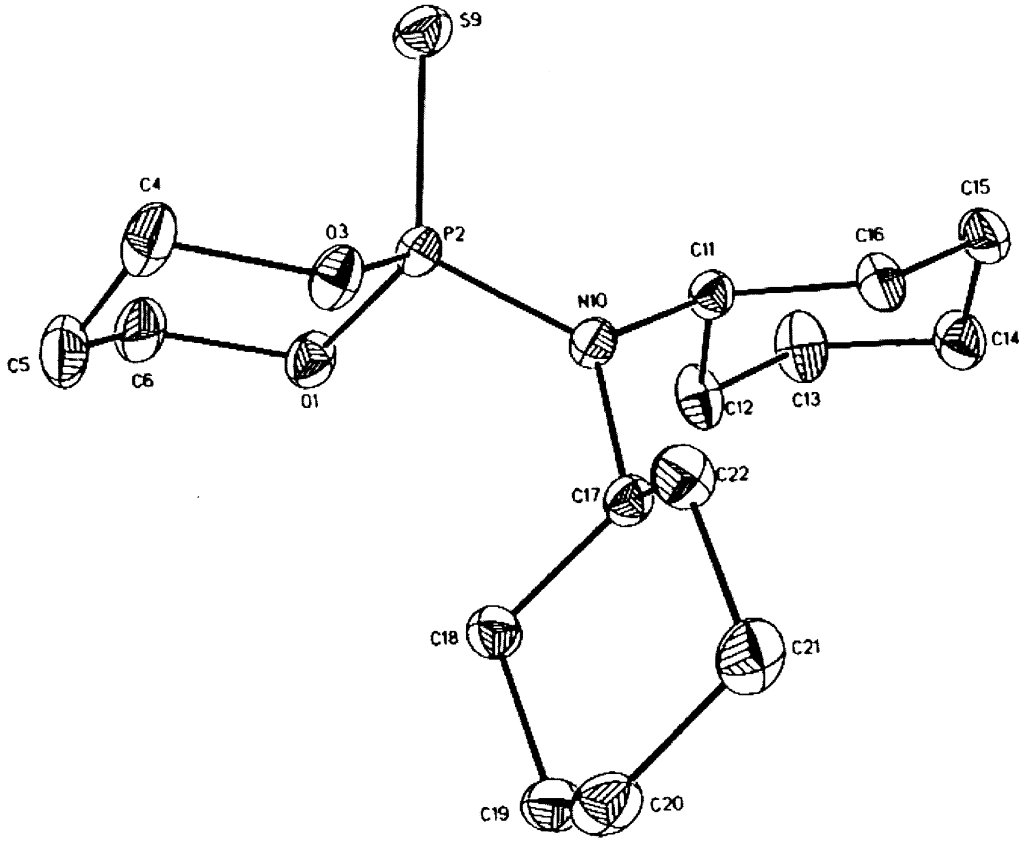

Figure 3. ORTEP drawing of 2-dicyclohexylamino-2-thio-1,3,2λ^{5}-dioxaphosphinane (**1**).

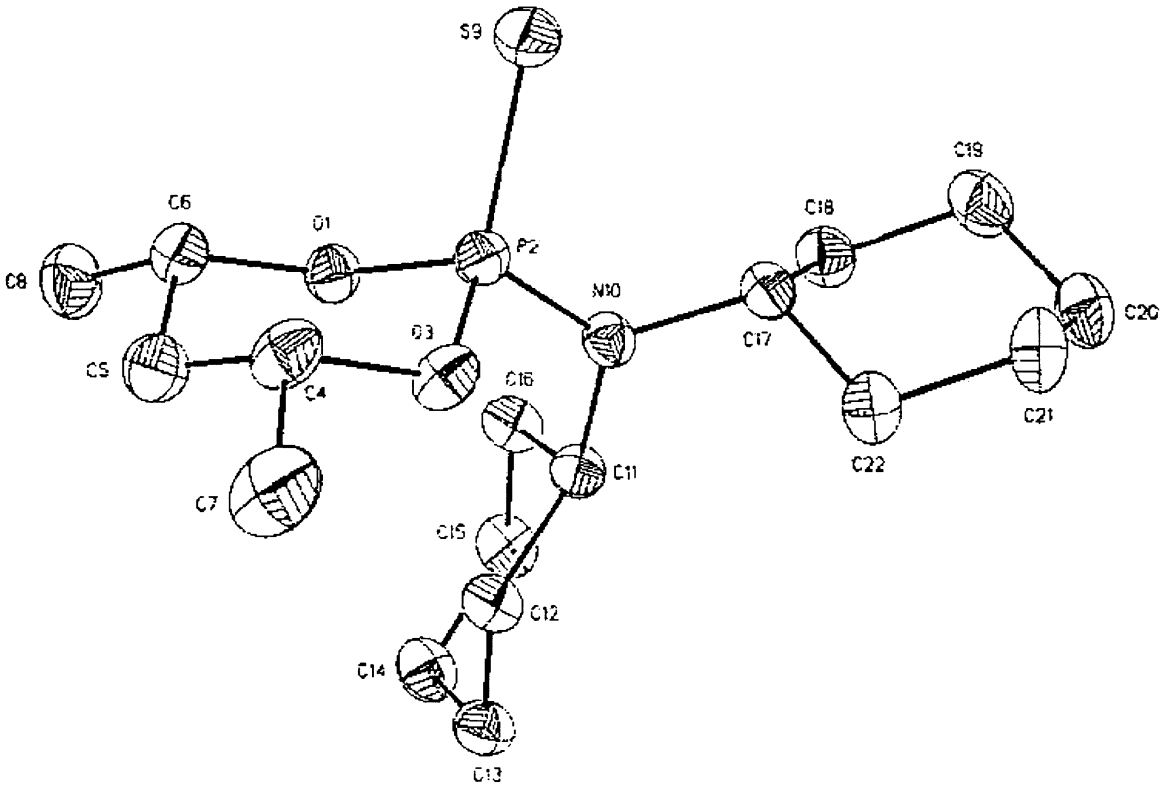

Figure 4. ORTEP drawing of *eq*-2-dicyclohexylamino-2-thio-*cis*-4,6-dimethyl-1,3,2λ^5-dioxaphosphinane (*eq-cis*-**2**).

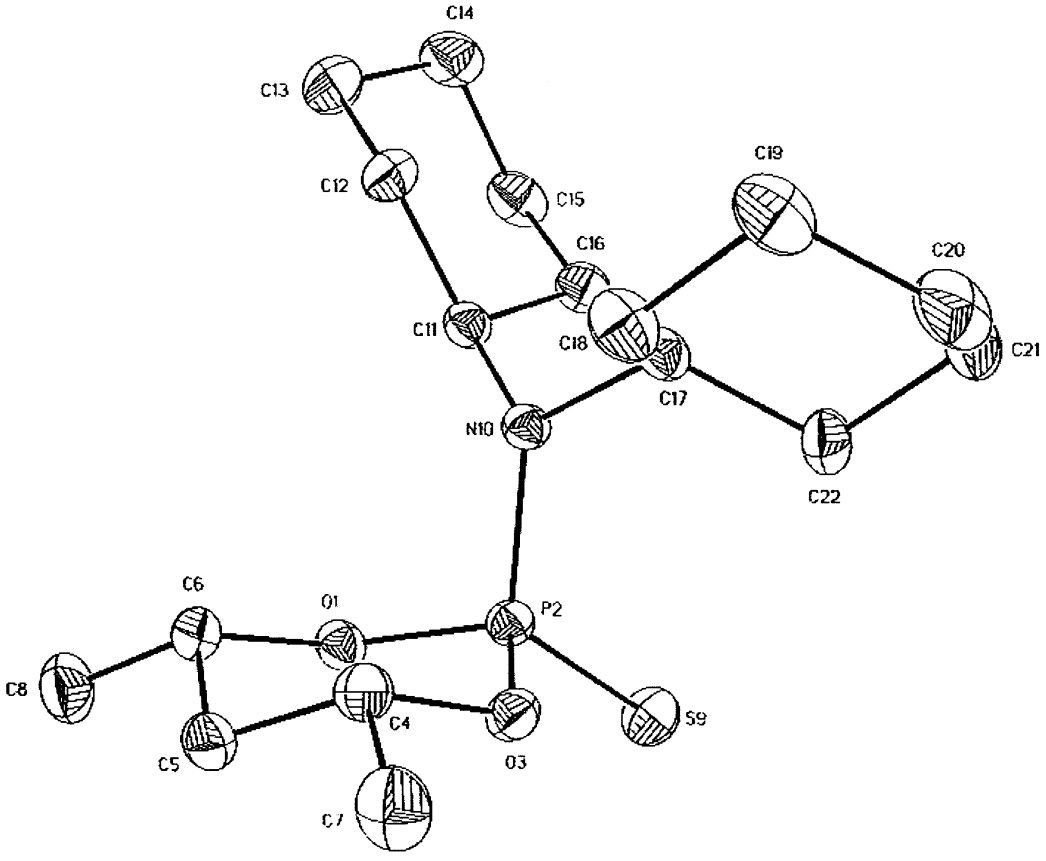

Figure 5. ORTEP drawing of *ax*-2-dicyclohexylamino-2-thio-*cis*-4,6-dimethyl-1,3,2λ^5-dioxaphosphinane (*ax-cis*-**2**).

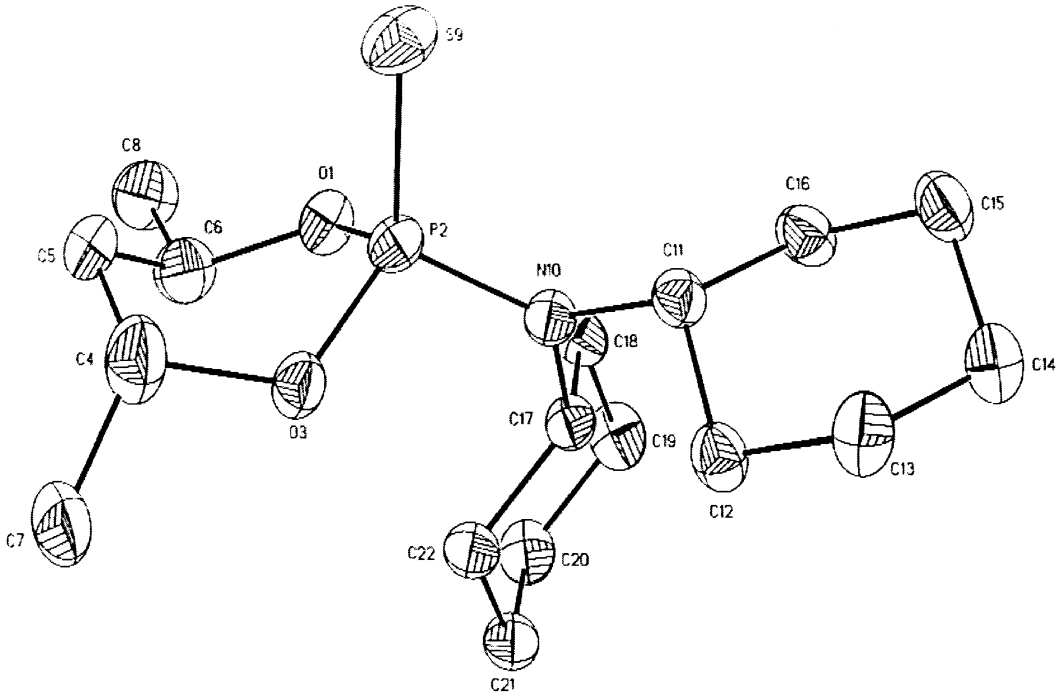

Figure 6. ORTEP drawing of 2-dicyclohexylamino-2-thio-*trans*-4,6-dimethyl-1,3,2λ^5-dioxaphosphinane (*trans*-**2**), molecule **A**.

respectively. These discrepancies and the fact that calculations using Eq. (1) were not reproducible, led us to discard that in solution, compound *trans*-**2** is in a rapid equilibrium chair–inverted chair (Scheme 7b). Taking into account the high flexibility of the 1,3,2-dioxaphosphinane ring,[3,7] an alternate explanation is that *trans*-**2** is not in a chair but in a conformational distortable or flippable system with the twist being the preferred conformation (Fig. 1). Indeed, the fact that the vicinal coupling constants $^3J_{HH}$ are of an intermediate value between *anti* (~12 Hz) and *gauche* (2.5–4.5 Hz) arrangements [$^3J_{H4aH5a}$=7.0 Hz, $^3J_{H4aH5e}$= 5.2 Hz, and $^3J_{H6eH5a}$=$^3J_{H6eH5e}$=4.7 Hz] suggests a twist as the most likely conformation (Fig. 1). Besides, the $^3J_{H4aP}$=3.5 Hz and $^3J_{H6eP}$=15.6 Hz of *trans*-**2** (Table 3), are very much similar to the ones found by Bentrude[30] for the $^3J_{HP}$ of the pseudoequatorial hydrogens Ha and Hd (18 and 15 Hz, respectively), and the pseudoaxial hydrogens Hb and Hc (5.0 and 2.6 Hz, respectively) of the *cis*-2-oxo-2-

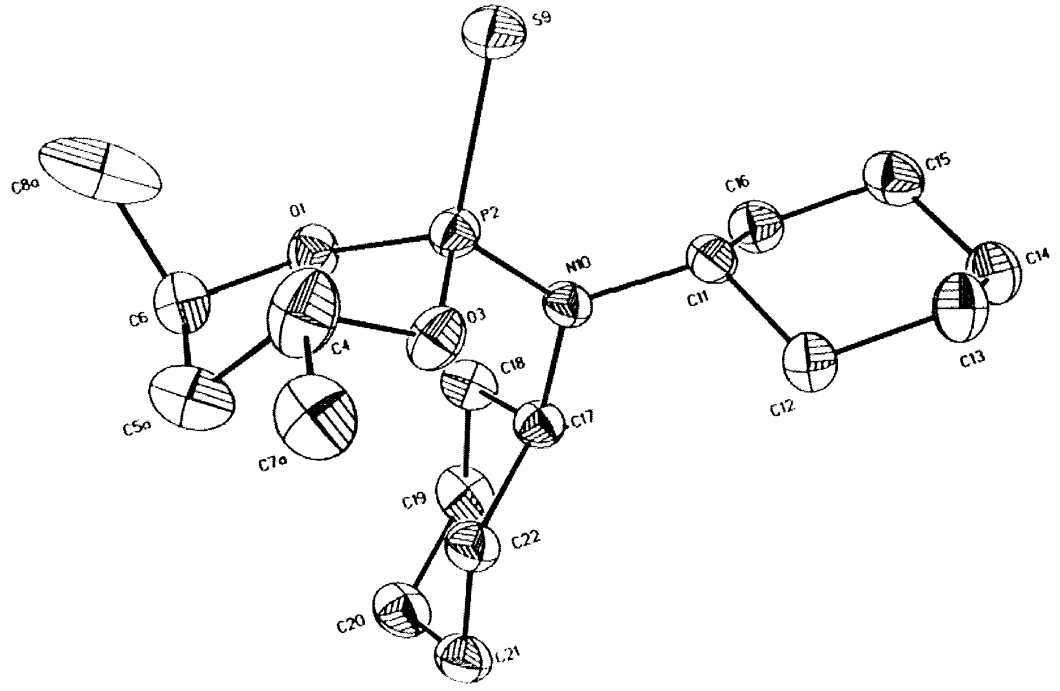

Figure 7. ORTEP drawing of 2-dicyclohexylamino-2-thio-*trans*-4,6-dimethyl-1,3,2λ^5-dioxaphosphinane (*trans*-**2**), molecule **B**.

dimethylamino-3-phenyl-5-*tert*-butyl-1,3,2λ^5-oxazaphosphinane of Fig. 2, which adopts preferentially a twist conformation in solution and in solid state.

Similarly, *trans*-**2** exhibit in the solid state distorted twisted boat/half-chair (chaise loungue) forms wherein the amino group is pseudoequatorial. Here, it is evident that the 1,3-synaxial Me/S interaction is of repulsive origin. Whether this interaction is due to steric compression or not, is a point of discussion in *structural analysis* given later. What is clear from these results is that the flexible 1,3,2λ^5-dioxaphosphinane ring in *trans*-**2** has a less energy demanding route than cyclohexane to relieve the intramolecular van der Waals repulsive compression of the nonbonded substituents. In other words, the behavior in a flexible 1,3,2-dioxaphosphinane ring may be due to the fact that the compromise between the intraannular torsional strain and the Baeyer strain, is any other but the one in cyclohexane.[31]

Structural analysis. During our studies, we were able to obtain X-ray quality crystals of **1** and the configurational isomers of **2**. The ORTEP drawings of them are shown in Figs. 3–7. Data collection and refinement parameters, bond distances, bond angles, and torsion angles are provided in Tables 4–7.

Thiophosphoramidates **1**, and *ax-cis*-**2** crystallized in the not very common[33] triclinic space group *P*-1, whereas *eq-cis*-**2** and *trans*-**2** crystallized in the monoclinic space group $P2_1/c$. Disorder[34] was observed during the refinement of *trans*-**2**, in which a monomorphic model (a model without multiple site atomic positions) led to a large R_1=0.061. Thus, a dimorphous model with C5 (B_{11}=6.7 Å^2), C7 (B_{11}=7.5 Å^2) and C8 (B_{11}=7.1 Å^2) in two sites, was considered (supplementary material). This model led to R_1=0.048 after refinement with occupancies of the disordered sites in the ratio of 78:22, for molecule **A** (Fig. 6) and **B** (Fig. 7), respectively. The ORTEP diagrams for the **A** and **B** were obtained eliminating the fragment C7a, C5a and C8a first, and then the fragment C7, C5 and C8 with the aim of observing the two conformers easily.

The natural tendency of the dicyclohexylamino substituent to occupy the equatorial position in a chair dioxaphosphinane ring is observed in compound **1** (Fig. 3). The geometry at the phosphorus center is tetrahedral; the sum of the four angles at P is 437.18°, and the geometry at nitrogen is trigonal planar, the sum of the three angles at the N is 358.37° (Table 8). This situation is quite similar to the anancomeric *eq-cis*-**2** in which the molecule also adopts a chair conformation (Fig. 4) with no severe distortion caused by the buttressing effect of the methyl groups at C4 and C6 [bond angle (θ_{OCC5})=110.15° (mean) for **1** vs. 109.2° (mean) for *eq-cis*-**2**; and torsion angle (ω_{POCC5})=58.26° (mean) for **1** vs. 56.24° (mean) for *eq-cis*-**2**]. It is worthwhile to note that in this case there is not ring flattening in the OPO region as it is usually observed in the dioxaphosphinane ring, in chair conformation, of phosphates with the same configuration.[35]

Table 4. X-Ray crystal data for compounds **1** and **2**

	1	*eq-cis*-**2**	*ax-cis*-**2**	*trans*-**2**
Formula	$C_{15}H_{28}NO_2PS$	$C_{17}H_{32}NO_2PS$	$C_{17}H_{32}NO_2PS$	$C_{17}H_{32}NO_2PS$
FW	317.41	345.47	345.47	345.47
Crystal system	Triclinic	Monoclinic	Triclinic	Monoclinic
Crystal size (mm^3)	0.50×0.28×0.22	0.56×0.34×0.20	0.24×0.36×0.42	0.34×0.25×0.22
Space group	*P*-1	$P2_1/c$	*P*-1	$P2_1/c$
Radiation	Mo Kα	Mo Kα	Mo Kα	Mo Kα
Wavelength (Å)	0.71073	0.1073	0.71073	0.71073
a (Å)	6.4580(10)	12.701(3)	7.1240(10)	12.936(3)
b (Å)	8.895(2)	10.428(2)	8.877(2)	10.400(2)
c (Å)	15.769(3)	14.893(3)	16.645(3)	14.515(3)
α (°)	101.96(3)	90.00	95.25(3)	90.00
β (°)	93.19(3)	100.27(3)	98.27(3)	98.53(3)
γ (°)	108.30(3)	90.00	110.03(3)	90.00
V (Å^3)	842.7(3)	1940.9(7)	967.4(3)	1931.2(7)
Z	2	4	2	4
2θmax (°)	50	50	50	50
d_{calcd} (Mg m^{-3})	1.251	1.182	1.186	1.188
Absorption coefficient (mm^{-1})	0.289	0.256	0.257	0.257
No. of reflections collected	3442	7197	3694	3540
No. of independent reflections	2961	3414	3397	3393
No. of observed reflections	2402	2323	2806	1841
R_1 [$F>4\sigma(F)$]	0.0371	0.035	0.0372	0.0477
wR_2	0.0959	0.0955	0.0994	0.1366
R_1 (all data)	0.0500	0.0707	0.0473	0.1163
wR_2	0.1049	0.1104	0.1071	0.1682
GOF on F^2	1.021	1.001	1.047	1.079
Max. shift for final cycle of least-squares	0.000	0.000	0.000	0.000
Δ/σ	0.000	0.000	0.001	0.000
Max. peak in final difference syntheses (e/Å^3)	0.306	0.178	0.292	0.334
Max. difference hole (e/Å^3)	−0.253	−0.216	−0.314	−0.308

Standard deviations are in parentheses.

Table 5. Selected bond lengths (Å) for **1** and **2**

	1	*eq-cis*-**2**	*ax-cis*-**2**	*trans*-**2**	
				Molecule **A**	Molecule **B**
O1–P2	1.593(2)	1.585(2)	1.5817(14)	1.573(2)	1.573(2)
O3–P2	1.5917(15)	1.588(2)	1.5836(14)	1.583(2)	1.583(2)
N10–P2	1.629(2)	1.627(2)	1.6609(15)	1.629(3)	1.629(3)
S9–P2	1.9271(9)	1.9277(9)	1.9212(7)	1.9294(13)	1.9294(13)
O1–C6	1.466(3)	1.468(3)	1.470(2)	1.479(5)	1.479(5)
O3–C4	1.462(3)	1.466(3)	1.474(2)	1.464(4)	1.464(4)
C4–C5	1.499(4)	1.495(3)	1.504(3)	1.520(6)	1.55(2)
C5–C6	1.503(4)	1.497(3)	1.510(3)	1.477(6)	1.54(2)
C6–C8	–	1.497(3)	1.507(3)	1.477(6)	1.50(2)
C4–C7	–	1.496(3)	1.503(3)	1.472(7)	1.48(2)
C11–N11	1.491(2)	1.487(3)	1.488(2)	1.889(4)	1.489(4)
C17–N10	1.494(2)	1.496(2)	1.498(2)	1.501(4)	1.501(4)

Standard deviations are in parentheses.

Table 6. Selected bond angles (θ) in deg for **1** and **2**

	1	*eq-cis*-**2**	*ax-cis*-**2**	*trans*-**2**	
				Molecule **A**	Molecule **B**
O1–P2–O3	102.45(9)	102.49(8)	105.52(7)	102.51(13)	102.51(13)
O1–P2–N10	106.53(9)	103.55(9)	105.08(8)	104.67(13)	104.67(13)
O1–C6–C5	109.9(2)	110.2(2)	109.63(15)	110.5(3)	120.5(7)
O3–C4–C5	110.4(2)	108.2(2)	109.31(15)	11.5(3)	96.8(7)
O2–P2–N10	113.02(7)	113.97(6)	109.49(6)	113.80(10)	113.80(10)
O1–P2–S9	113.58(7)	112.51(5)	111.70(6)	112.98(11)	112.98(11)
O3–P2–S9	113.58(7)	112.51(6)	111.70(6)	112.98(11)	112.98(11)
C4–O3–P2	114.50(13)	116.96(13)	118.17(11)	117.9(2)	117.9(2)
C6–O1–P2	115.90(14)	117.42(14)	121.29(11)	118.6(2)	118.6(2)
C6–C5–C4	112.4(2)	113.7(2)	112.6(2)	111.0(4)	106.0(10)
P2–N10–C11	117.72(13)	119.43(13)	117.06(11)	119.6(2)	119.6(2)
P2–N10–C17	124.36(13)	123.87(14)	121.44(12)	124.1(2)	121.1(2)
C11–N10–C17	116.29(15)	116.2(2)	114.98(13)	115.5(2)	115.5(2)
S9–P2–N10	116.42(7)	115.94(7)	119.35(6)	114.57(10)	114.57(10)

Standard deviations are in parentheses.

Table 7. Selected torsion angles (ω) in deg for **1** and **2**

	1	*eq-cis*-**2**	*ax-cis*-**2**	*trans*-**2**	
				Molecule **A**	Molecule **B**
S9–P2–O3–C4	67.31(16)	70.11(15)	−160.96(11)	65.21(27)	65.21(27)
N10–P2–O3–C4	−165.55(15)	−161.35(15)	68.53(14)	−167.59(26)	−167.59(26)
O1–P2–O3–C4	−54.91(17)	−52.73(16)	−42.07(14)	−57.69(28)	−57.69(28)
O1–C6–C5–C4	55.38(30)	54.96(26)	56.19(22)	−64.76(46)	48.14(1.20)
S9–P2–O1–C6	−68.22(17)	−71.56(15)	159.27(12)	98.87(24)	98.87(24)
N10–P2–O1–C6	162.72(16)	161.60(15)	−71.39(15)	−135.31(25)	−135.31(25)
O3–P2–O1–C6	54.39(17)	50.29(16)	38.92(15)	−23.48(27)	−23.48(27)
O3–P2–O1–C6	54.39(17)	50.29(16)	38.92(15)	−23.48(27)	−23.48(27)
P2–O3–C4–C5	59.38(24)	58.30(22)	55.04(19)	30.49(44)	82.08(70)
P2–O3–C4–C7	–	−177.85(16)	179.29(14)	158.95(35)	−169.60(68)
P2–O1–C6–C8	–	−177.79(16)	−170.38(14)	161.94(30)	103.20(1.06)
P2–O1–C6–C5	−57.15(25)	−54.18(22)	−47.55(20)	32.76(41)	−25.39(86)
C11–N10–P2–O1	93.43(16)	152.56(15)	−45.44(14)	155.53(22)	155.53(22)
C11–N10–P2–O3	−158.97(14)	−99.56(16)	−156.36(12)	−96.07(24)	−96.07(24)
C11–N10–P2–S9	−33.63(17)	26.98(17)	77.79(14)	30.18(26)	30.18(26)
C17–N10–P2–O1	−71.43(17)	−36.17(18)	164.29(13)	−35.33(27)	−35.33(27)
C17–N10–P2–O3	36.17(18)	71.71(17)	53.37(15)	73.07(26)	73.07(26)
C17–N10–P2–S9	161.51(14)	−161.75(14)	−72.48(15)	−160.68(21)	−160.68(21)

Standard deviations are in parentheses. Right-hand rule.[32]

Table 8. Structural properties of **1** and **2**

	1	*eq-cis*-**2**	*ax-cis*-**2**	*trans*-**2**	
				Molecule **A**	Molecule **B**
Geometry at phosphorus[a]	437.18	437.00	440.35	436.43	436.43
Geometry at nitrogen[b]	358.37	359.50	353.48	359.20	359.20
Baeyer strain[c]	110.93	111.50	112.75	112.0	110.40
Pitzer strain[d]	56.37	54.52	50.05	40.30	50.70
cos ω	0.55	0.58	0.64	0.76	0.63
$-\cos\theta/(1+\cos\theta)$	0.56	0.58	0.63	0.59	0.53

[a] Calculated as the sum of the bond angles (O1P2O3), [OP2N10 (mean)], [OP2S9 (mean)] and (S9P2N10) in deg.
[b] Calculated as the sum of the bond angles (P2N10C11), (P2N10C17), and (C11N10C17) in deg.
[c] Calculated as the average value of the bond angles (O1P2O3), (O1C6C5), (O3C4C5), (C4O3P2), (C6C5C4) and (C6O1P2) in deg.
[d] Calculated as the average absolute value of the torsion angles (O1P2O3C4), (O1C6C5C4), (O3P2O1C6), (O3C4C5C6), (P2O3C4C5) and (P2O1C6C5) in deg.

Summarized in Table 8 are also the Baeyer and Pitzer strain[31] for compounds **1** and *eq-cis*-**2** [calculated as the average of the internal bond angles (θ), and torsion angles (ω) of the dioxaphosphinane ring, respectively]. Remarkably, there is a very good correlation between the values of cos ω and $-\cos\theta/(1+\cos\theta)$,[36] being 0.55 vs. 0.56 for **1** and 0.58 vs. 0.58 for *eq-cis*-**2**. The agreement between these values indicates the propensity of the dioxaphosphinane ring in a chair conformation, to fulfill the same global requirements of cyclohexane, with regard to the compromise between bond angles and torsion angles (imposed by the constraint of the ring) which leads to the minimum strain in the molecule. Thus, the observed decrease in the bond angles [111.2° (mean value of the Baeyer strain for **1** and *eq-cis*-**2** in Table 8) against 112.4° (the bond angle in propane)] brings with it a decrease in the intraannular torsion angles [55.4° (mean value of the Pitzer strain for **1** and *eq-cis*-**2** in Table 8) instead of 60° (the tetrahedral angle)]. It is important to stress that although the average analysis of the dioxaphosphinane ring is in-line with the one in cyclohexane, an analysis of the individual angles does not necessarily have the same scope, because in the dioxaphosphorinane ring, there are striking differences between the internal bond angles COP (~115°), OPO (~102.5°) and CCC (~113°), rendering the chair with an outline which lacks of perpendicular symmetry, wherein the oxygens tend to be flat edges, and the phosphorus a puckery end.

As mentioned earlier, the 1,3,2-dioxaphosphinane **1** with an equatorial amino substituent is thermodynamically more stable than the corresponding isomer with the amino group in axial position. In order to rationalize this behavior, we compared the structural data of *eq-cis*-**2** (Fig. 4) with the ones of *ax-cis*-**2** (Fig. 5). Indeed, by doing an individual examination of the bond lengths and bond angles, we find that the average COP angle in *ax-cis*-**2** is around 119.7° whereas in *eq-cis*-**2** is around 117.2°; these angles are substantially larger than the tetrahedral, as a matter of fact very close to the trigonal, indicating that the *endo*-cyclic oxygens in the dioxaphosphinane ring are prone to change their hybridization from sp^3 to sp^2. The opening of the COP angle in the *ax-cis*-**2** isomer can be attributed to the repulsive 1,3-synaxial $H/N(C_6H_{11})_2$ interaction whereupon the molecule minimizes the strain introduced by the intramolecular repulsive van der Waals compression of the nonbonded substituents. Evidently, in this case, there is a flattening of the OPO region [($\omega_{PO3C4C5}$)=55.04°; and ($\omega_{PO1C6C5}$)=−47.55°] which confirms the presence of the repulsive 1,3-synaxial interaction, even though some puckering is conserved at the phosphorus center (θ_{O1P2O3}=105.5°). In the conformation shown in Fig. 5, in which the nitrogen also display a trigonal geometry (Table 8), the electron pair at nitrogen is thus in a p orbital confronting the ring and therefore the steric 1,3-synaxial interaction H/NR_2 is not highly appreciated; however since the P–N bond is prevented from free rotation; then, it is clear that the *ax-cis*-**2** isomer is disfavored by entropy, and with a high probability by enthalpy too [note by the data in Table 8 that the average values of the Baeyer and the Pitzer strain for this compound, also compromise with themselves in such a way that the global strain of the heterocycle is minimized (as discussed earlier)].

Data on bond distances (Table 5) indicate clearly that the *exo*-anomeric effect $n_\pi N-\sigma^*_{P-O}$[16] does participate in the stabilization of the amino group $N(C_6H_{11})_2$ in the equatorial position of the thiophosphoramidates **1** and *eq-cis*-**2**, since the N10–P2 bond is indeed shorter (1.629 and 1.627 Å, respectively) than in *ax-cis*-**2** (1.661 Å); and although there is no a substantial elongation of P2–O1(3) in **1** and *eq-cis*-**2** [1.590 Å (mean), and 1.587 Å (mean), respectively] vs. 1.583 Å (mean) in *ax-cis*-**2**, the fact that the free electron pair at nitrogen is located in a p orbital, which is in an antiperiplanar relationship to one of the *endo*-cyclic P–O bonds (see the torsion angles of the cyclohexane rings in Table 7, i.e: $\omega_{C17NPO1}$=36.17°, $\omega_{C11NPO3}$=99.56°; or $\omega_{C17NP03}$=71.71°, $\omega_{C11NPO1}$=152.56° for *eq-cis*-**2**) confirms that this interaction is a plausible mechanism for the stabilization of equatorial amino substituted thiophosphoramidates. Besides, the *exo*-anomeric interaction is indeed neglected in axial thiophosphoramidates as it is shown for example in the anancomeric *ax-cis*-**2** isomer since the lone pair at nitrogen is constrained to be in a parallel (although non antiperiplanar) relationship to any of the PO bonds ($\omega_{C11NPS9}$=77.79°, $\omega_{C17NPS9}$=−72.48°), as observed in Fig. 5.

The fact that there is no elongation of P2–O1(3) in **1** or *eq-cis*-**2** as compared with *ax-cis*-**2**, is very likely also a result of the participation of the *endo*-anomeric interaction $n_\pi O-\sigma^*_{P=S}$[17] that will tend to shorten the P–O *endo*-cyclic bond

according to the participation of the resonance shown in Scheme 4. In support, a small elongation of the P═S bond in **1** or *eq-cis*-**2** compared with *ax-cis*-**1** [P═S in **1** is 1.927 Å and in *eq-cis*-**2** 1.928 Å vs. P═S in *ax-cis*-**2**, which is 1.921 Å] was observed. Nevertheless, the *exo*-anomeric effect remains as the most likely mechanistic alternative to explain the increased stabilization of the equatorial amino substituent in the conformational equilibrium of **1**, because as it has been pointed out by Bentrude[17a] and Verkade,[17b] the lone pair on the heteroatom of a P═X group (being X═O, S) may cause bonding electron repulsion when it is in the axial position, weakening the participation of the $n_{\pi}O-\sigma^{*}_{P=X}$ *endo*-hyperconjugative interaction in the stabilization of the equatorial amino group of phosphoramidates or their thio analogs.

Perhaps the most interesting system of all the others presented here is the *trans*-**2** isomer, since the conformational analysis in solution and in solid state indicates the participation of twist and/or boat conformations. This finding provides extra evidence of the high flexibility of the dioxaphosphinane ring observed for some analogous phosphorus heterocycles.[3,7,37–39] Besides, an important feature in the crystallographic structure of *trans*-**2** is the fact that even in solid state, the molecule exhibits atomic displacement adopting twisted boat and half-chair conformations (molecules **A** and **B** of Figs. 6 and 7, respectively), thereby providing additional evidence that the conformational interconversion barrier of this dioxaphosphinane ring is remarkably small. Atomic displacements in crystals have also been observed for strained cyclohexane fragments of bicyclo systems in equilibrium.[40]

It is worth noting that in both conformations found in the solid state of *trans*-**2**, the amino $N(C_6H_{11})_2$ group is in the pseudoequatorial position (Figs. 6 and 7), presumably because they are benefiting from the *exo*-anomeric interaction [the lone pair at nitrogen remains antiperiplanar to a PO *endo*-cyclic bond (molecules **A** and **B**: $\omega_{C11NPS9}$= 30.18°, and $\omega_{C17NPS9}$=160.68° for both of them (Table 7)]. In order to compare which of the two conformations of the solid state was closer to the conformation observed in solution (Fig. 1), we decided to locate H4a and H4b, as well as H6a and H6b from difference Fourier map and refine them to calculate the dihedral angles of the segment H4a–C4–O3–P, H6a–C6–O1–P for the twisted boat and H4b–C4–O3–P, H6b–C6–O1–P for the half-chair conformations. The calculated values for the first pair of angles were −49.1° and −139.7°, while those for the half-chair were −83.6° and −82.9°. Taking into account that in solution the coupling constants $^{3}J_{H4aP}$ and $^{3}J_{H6eP}$ are equal to 3.5 and 15.6 Hz, respectively (Table 3), the half-chair conformation is discarded because being the dihedral angles very close to one another (C_2 symmetry), the two $^{3}J_{HP}$ must have had also similar values in between them. On the other hand, the calculated dihedral angles for the twisted boat are in better agreement with the $^{3}J_{HP}$ values obtained by NMR.

In addition, it is observed that there is a repulsive 1,3-synaxial Me/S interaction judged by the increase of the COP intraannular angle to an almost trigonal one [118.25° (mean) for the twisted boat, and for the half-chair

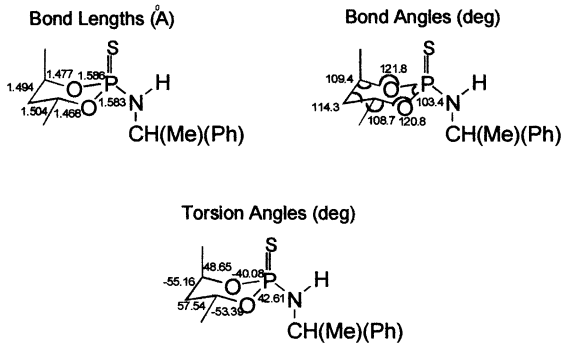

Scheme 8.

(molecules **A** and **B** in Figs. 6 and 7 respectively)]. Of course in molecule **B**, there is a compromise between the flattening at the oxygen centers, and the steric hindrance of the cyclohexyl groups with the methyl at C7a, which takes place when the amino group tend to pass from the pseudoequatorial to the pseudoaxial position [some of the nonbonded (C–H) interactions between the methyl and cyclohexyl groups are in the range of 3–4 Å, demonstrating that the van der Waals contact between the two hydrogen atoms: one at Me (C7a) and the other at one of the cyclohexyl groups indeed exists (a complete list of the carbon–hydrogen bond contacts, between 0.5 and 5.0 Å, is provided in the supplementary material)].

It is interesting to compare these conformations with the one adopted by the analog (4*S*,6*S*,11*R*)-(+)-*trans*-4,6-dimethyl-2-(1-phenylethylamino)-2-thio-1,3,2λ^{5}-dioxaphosphinane (**3**) in the solid state[41] (Scheme 8). As observed, **3** adopts a chair conformation with the amino substituent in the equatorial position. The molecule displays ring flattening in the OPO end [(ωP03C4C5)=48.65°; and (ωPO1C6C5)=−53.39°] which confirms interestingly, that there is also a repulsive 1,3-synaxial Me/S interaction as such observed for *trans*-**2** (as discussed earlier). The origin of this interaction cannot only be ascribed to a repulsive compression (steric hindrance) because the nonbonded distances between the hydrogens in the methyl group at C8 and the sulfur are 3.127, 3.693, and 4.591 Å, larger than the sum of the van der Waals radii of hydrogen and sulfur (3.0 Å).[42] Thus, the 1,3-synaxial Me/S interaction is perhaps an example of the phenomena that has been named kinetic energy pressure or restriction on electron-movement.[43]

More strikingly is the finding that although **3** is very closely related structurally to *trans*-**2**, the former adopt a chair and the second two distorted conformations. A thorough comparison of the structural parameters of both molecules has given rise to the observation that there is a difference between the *exo*-cyclic NPS bond angle (in *trans*-**2** is equal to 114.6° and in **3** to 112.6°), suggesting that the geminal effect[31] of the dicyclohexylamino group on sulfur is stronger than the one caused by the 1-phenylethylamino group, therefore the buttressing interaction [NR_2/S→Me (C8)] in *trans*-**2** is stronger than the buttressing interaction [NHR/S→Me(C8)] in **3**, so that only *trans*-**2** is forced to deform-out of the C4C5C6 region, in order to release such strain in the molecule.

4. Conclusions

The conformational properties of isomeric dicyclohexylamino substituted 1,3,2-dioxaphosphinanes are analyzed in light of their behavior in solution and their structural data obtained by X-ray analysis.

The dicyclohexylamino substituent in **1** prefers the equatorial position for at least a ΔG^0 (25°C)=−3.27 kcal/mol (N=0.996) in chloroform, as well as in solid state as can be observed from its X-ray structure. The origin of this preference rest mainly on the attractive *exo*-anomeric $n_{\pi}N-\sigma^*_{P-O}$ interaction and the repulsive H/N(C_6H_{11}) interaction more than the *endo*-anomeric $n_{\pi}O-\sigma^*_{P=S}$ interaction. The anancomeric *ax-cis*-**2** and *eq-cis*-**2** adopt chair conformations in solution and in solid state, regardless of the large size of the amino substituent. On the other hand, *trans*-**2** isomer adopts a twist conformation in solution and a mixture of twisted boat/half-chair conformations in equilibrium in solid state. In any of these two conformations, there are sizeable Me/N(C_6H_{11})$_2$ and Me/S repulsive constraints.

The main difference between the conformational behavior of substituted cyclohexanes as compared with 1,3,2-dioxaphosphinanes, is that the heterocycle has the ability of releasing any intramolecular repulsive compression strain by means of a substantial change in the geometry of the ring. This ability is due to the aptitude of the *endo*-cyclic oxygens to change from sp^3 to sp^2 hybridization in the phosphorus heterocycle.

5. Experimental

Melting points are uncorrected. Nuclear magnetic resonance spectra were recorded on Jeol Eclipse 400 and Bruker Avance 300 spectrometers in $CDCl_3$ (δ 7.26, ^1H; δ 77.0, ^{13}C), ^1H at 399.8 and 300.1 MHz, ^{13}C at 100.5 and 75.5 MHz, and ^{31}P at 161.8 and 121.5 MHz, respectively. Phosphorus NMR spectra are reported in ppm downfield (+) from 85% H_3P0_4 used as external standard. Mass spectra (EI) were measured on a Hewlett Packard 5989 Å spectrometer using electron impact (EI) at 70 eV. The reactions were performed under an atmosphere of nitrogen in oven-dried glassware. Solvents and solutions were transferred by syringe-septum and cannula techniques. Solvents for the reactions: diethyl ether and toluene, were of reagent grade and were dried and distilled immediately before use from sodium/benzophenone. Triethylamine was dried and distilled from $LiAlH_4$. Products were purified by flash column chromatography on silica gel 230–400 mesh. The R_f of all compounds were determined in a solution of 80% *n*-hexane/ethyl acetate. Yields are given for crude and isolated products. Microanalyses were performed by Galbraith Laboratories, Inc., Knoxville, TN.

n-Hexane was used for recrystallization of all samples, affording crystals suitable for X-ray diffraction analysis. Crystallographic work was performed in an Enraf-Nonius CAD-4 diffractometer. Data collection: CAD-4 Software.[44] Cell refinement: CAD-4 Software. Data reduction: JANA98[45] The structures were solved by direct methods SHELXS86[46] and refined with SHELXL93[47] or SHELXL97[48]. Molecular graphics: XPMA[49] and dihedral angles: PARST 95.[50]

5.1. General procedure for the preparation of thiophosphoramidates 1 and 2

In a three-necked 2.0 L flask, fitted with dropping funnel, a stir bar, and rubber septa, were placed 0.13 mol of the corresponding diol, 21.0 mL (0.26 mol) of pyridine, and 1.3 L of dry diethyl ether. The solution was stirred at 0°C and 11.3 mL (0.13 mol) of phosphorus trichloride in 200.0 mL of diethyl ether were added slowly through the dropping funnel. The resulting suspension was evaporated in a rotary evaporator and transferred via a filter-tipped cannula to a dropping funnel that contained 200.0 mL of dry toluene. The funnel was previously set in another 2.0 L, three-necked flask, equipped with stir bar, and rubber septa which contained 25.9 mL (0.13 mol) of dicyclohexylamine and 18.1 mL (0.13 mol) of triethylamine in 1.0 L of dry toluene. The solution in the funnel was added dropwise, resulting in precipitation of a white solid (triethylammonium chloride). The solid was filtered off through a filter tipped cannula and the filtrate added to a 2.0 L flask, equipped with a stir bar and reflux condenser, into which it was added 4.17 g (0.13 mol) of elemental sulfur. The mixture was heated under reflux for 24 h. After cooling, the suspension was concentrated under vacuum and the residue washed with 600.0 mL of an aqueous solution of 10% sodium bicarbonate. The product was extracted with methylene chloride and the organic layer was dried over sodium sulfate. The solvent was removed with a rotary evaporator to yield a yellow oil. Purification of the crude product was accomplished by flash chromatography (hexane/ethyl acetate).

5.1.1. 2-Dicyclohexylamino-2-thio-1,3,2λ^5-dioxaphosphinane 1. According to the general procedure described earlier, 9.4 mL (0.13 mol) of 1,3-propanediol was treated with phosphorus trichloride followed by dicyclohexylamine and elemental sulfur to give 21.79 g (52.9%) of the crude product. Flash chromatography (hexane–ethyl acetate 95:5) of 1.81 g of the oily residue afforded 0.21 g (11.5% yield, R_f=0.31) of white crystals of mp 97–99°C. ^1H NMR δ 1.09 (dtt, J=13.2, 12.7, 3.4 Hz, 2H), 1.27 (dtt, J=13.8, 12.9, 3.2 Hz, 4H), 1.55 (m, 1H), 1.58–1.70 (m, 14H), 2.20 (dtt, J=14.4, 12.9, 4.9, 1H), 3.41 (dtt, J=20.1, 12.1, 3.5 Hz, 2H), 4.20 (ddt, J=25.3, 10.3, 4.9 Hz, J=2.3 Hz, 2H), 4.71 (dddd, J=12.9, 10.3, 4.5, 2.4 Hz, 2H); ^{13}C NMR δ 25.8 (s), 26.7 (d, J=6.6 Hz), 27.0 (s), 33.5 (d, J=1.4 Hz), 57.4 (d, J=5.4 Hz), 66.6 (d, J=6.1 Hz); ^{31}P NMR δ 72.7; MS (*m/z*) 317 (M^+), 284 (M^+-33), 248 (M^+-69), 234 (M^+-83), 179 (M^+-138), 105 (M^+-212), 98 (M^+-219), 41 (M^+-276). Anal. Calcd for $C_{15}H_{28}O_2PNS$: C, 56.75; H, 8.89. Found: C, 57.21; H, 8.84.

5.1.2. 2-Dicyclohexylamino-2-thio-4,6-dimethyl-1,3,2λ^5-dioxaphosphorinane 2. According to the general procedure described earlier, 0.13 mol of *meso* and *rac*-2,4-pentanediols (55:45)[51] were treated with phosphorus trichloride followed by dicyclohexylamine and elemental sulfur to give 21.12 g (47.1%) of a mixture of isomers. Flash chromatography (hexane–ethyl acetate 98:2) of 6.50 g of

the crude product afforded 0.08 g (1.2% yield) of *eq-cis*-**2**, 0.49 g (7.5% yield) of *ax-cis*-**2**, and 0.74 g (11.4% yield) of *trans*-**2**.

eq-cis-**2**: R_f=0.39; mp 112°C; ^{1}H NMR 1.07 (dtt, *J*=13.2, 12.4, 3.2 Hz, 2H), 1.21–1.30 (m, 4H), 1.31 (dd, *J*=6.1, 1.6 Hz, 6H), 1.53 (dt, *J*=13.9, 11.7 Hz, 1H), 1.60 (m, 4H), 1.69 (dq, *J*=13.9, 2.2 Hz, 1H), 1.72–1.85 (m, 10H), 3.46 (dtt, *J*=19.9, 11.3, 4.9 Hz, 2H), 4.79 (dqt, *J*=11.7, 6.1, 2.2 Hz, 2H); ^{13}C NMR δ 22.4 (d, *J*=9.9 Hz), 25.6 (s), 26.7 (s), 33.2 (s), 41.3 (d, *J*=3.8 Hz), 57.1 (d, *J*=4.6 Hz), 72.7 (d, *J*=5.4 Hz); ^{31}P NMR δ 71.9; MS (*m/z*) 345 (M^+), 312 (M^+-33), 262 (M^+-83), 230 (M^+-115), 194 (M^+-151), 180 (M^+-165), 133 (M^+-212), 98 (M^+-247), 55 (M^+-290), 41 (M^+-304). Anal. Calcd for $C_{17}H_{32}O_2PNS$: C, 59.10: H, 9.33. Found: C, 59.62: H, 9.52.

ax-cis-**2**: R_f=0.20; mp 117.5–119°C; ^{1}H NMR δ1.08 (dtt, *J*=12.9, 12.9, 3.6 Hz, 2H), 1.28 (dtt, *J*=13.3, 12.9, 3.3 Hz, 4H), 1.39 (dd, *J*=6.3, 1.5 Hz, 6H), 1.57–1.67 (m, 6H), 1.69 (dq, *J*=14.3, 2.2 Hz, 1H), 1.76–1.84 (m, 4H), 1.88–1.95 (m, *J*=11.1 Hz, 4H), 2.01 (dt, *J*=14.3, 11.5 Hz, 1H), 3.17 (dtt, *J*=17.4, 12.2, 3.5 Hz, 2H), 4.47 (dqt, *J*=11.5, 6.3, 2.2 Hz, 2H); ^{13}C NMR δ 22.4 (d, *J*=7.7 Hz), 25.7 (s), 26.8 (s), 33.3 (d, *J*=3.1 Hz), 39.8 (d, *J*=7.7 Hz), 57.0 (d, *J*=3.8 Hz), 75.0 (d, *J*=8.5 Hz); ^{31}P NMR δ 67.0; MS (*m/z*) 345 (M^+), 312 (M^+-33), 262 (M^+-83), 230 (M^+-115), 180 (M^+-165), 133 (M^+-212), 98 (M^+-247), 69 (M^+-276), 41 (M^+-304). Anal. Calcd for $C_{17}H_{32}O_2PNS$: C, 59.10; H, 9.33. Found: C, 59.04; H, 9.51.

trans-**2**: R_f=0.36; mp 87–89°C; ^{1}H NMR δ 1.05 (dtt, *J*=12.9, 12.6, 3.1 Hz, 2H), 1.19–1.31 (m, 4H), 1.35 (dd, *J*=6.9, 1.7 Hz, 6.2 Hz, 3H), 1.60 (d, *J*=6.2 Hz, 3H), 1.53–1.85 (m, 14H), 1.89 (dddd, *J*=14.2, 7.0, 4.7, 1.2 Hz, 1H), 1.93 (m, 1H), 3.36 (dtt, *J*=19.9, 10.1, 5.0 Hz, 2H), 4.61 (dqt, *J*=15.6, 6.2, 4.7 Hz, 1H), 4.90 (dqdd, *J*=7.0, 6.9, 5.2, 3.5 Hz, 1H); ^{13}C NMR δ 21.9 (d, *J*=2.3 Hz), 22.4 (d, *J*=9.2 Hz), 25.6 (s), 26.8 (s), 33.2 (d, *J*=3.1 Hz), 37.8 (d, 7.7 Hz), 57.1 (d, *J*=5.4 Hz), 69.4 (d, *J*=5.4 Hz), 74.5 (d *J*=6.9 Hz); ^{31}P NMR δ 68.0; MS (*m/z*) 345 (M^+), 312 (M^+-33), 262 (M^+-83), 194 (M^+-151), 180 (M^+-165), 133 (M^+-212), 98 (M^+-247), 55 (M^+-290), 41 (M^+-304). Anal. Calcd for $C_{17}H_{32}O_2PNS$: C, 59.10; H, 9.33. Found: C, 59.61; H, 9.54.

Acknowledgements

We are in debt with the reviewers for helpful comments and explanations that assisted us to clarify some of the results of this work. Financial support came from CONACyT (Mexico) Grant 32221-E.

References

1. Carruthers, M. H. *Science* **1985**, *230*, 281.
2. Feigl, D. M.; Hill, J. W. *General, Organic, and Biological Chemistry. Foundations of Life*; Burguess Publishing: New York, 1983; chapter 18.
3. Bentrude, W. G. Steric and Stereoelectronic Effects in 1,3,2-Dioxaphosphorinanes. In *Conformational Behavior of Six Membered Rings. Analysis, Dynamics and Stereoelectronic Effects*; Juaristi, E., Ed.; VCH: New York, 1995; pp. 245–293.
4. (a) Edmundson, R. S.; Mitchell, E. W. *J. Chem. Soc. (C)* **1968**, 2091. (b) Edmundson, R. S. *J. Chem. Soc., Perkin Trans. 1* **1972**, 1660.
5. (a) Nifant'ev, É. E.; Borisenko, A. A.; Sergeev, N. M.; Ivanova, N. A. *Zh. Obshch. Khim.* **1970**, *40*, 1420. (b) Nifant'ev, É. E.; Borisenko, A. A. *Zh. Obshch. Khim.* **1977**, *47*, 482.
6. Bouchu, D.; Dreux, J. *Tetrahedron Lett.* **1976**, 3151.
7. Maryanoff, B. E.; Hutchins, R. O.; Maryanoff, C. A. *Top. Stereochem.* **1979**, *11*, 187.
8. (a) Bentrude, W. G.; Tan, H.-W. *J. Am. Chem. Soc.* **1973**, *95*, 4666. For similar analysis in isosteres see for example (b) Bentrude, W. G.; Setzer, W. N.; Sopchik, A. E.; Bajwa, G. S. *J. Am. Chem. Soc.* **1986**, *108*, 6669.
9. Bentrude, W. G.; Yee, K. C. *J. Chem. Soc. Chem. Commun.* **1972**, 169.
10. (a) Squillacote, M.; Sheridan, R. S.; Chapman, O. L.; Anet, F. A. L. *J. Am. Chem. Soc.* **1975**, *97*, 3244. (b) Kellie, G. M.; Ridell, F. G. *Top. Stereochem.* **1974**, *8*, 225.
11. (a) Eliel, E. L.; Knoeber, M. C. *J. Am. Chem. Soc.* **1968**, *90*, 3444. (b) Riddell, F. G.; Robinson, J. T. *Tetrahedron* **1967**, *23*, 3417. (c) Pihlaja, K. *Acta Chem. Scand.* **1948**, *22*, 716.
12. Van Nuffel, P.; Van Alsenoy, C.; Lenstra, A. T. H.; Geise, H. J. *J. Mol. Struct.* **1984**, *125*, 1.
13. Bentrude, W. G.; Hargis, J. H. *J. Am. Chem. Soc.* **1970**, *92*, 7136.
14. (a) Mosbo, J. A.; Verkade, J. G. *J. Org. Chem.* **1977**, *42*, 1549. (b) Mosbo, J. A. *Org. Magn. Reson.* **1978**, *11*, 281.
15. Muiphy, P. C.; Tebby, J. C. $d\pi-p\pi$ Bonding Effects on ^{31}P NMR Chemical Shift of *N*-Aryliminophosphoranes. In *Phosphorus Chemistry, Proceedings of the 1981 International Conference*; Quin, L. D., Verkade, J. G., Eds.; *ACS Symposium Series*; ACS: Washington, DC, 1981; Vol. 171, p. 573.
16. Arshinova, R. P. *Russ. Chem. Rev.* **1984**, *53*, 351.
17. (a) Ref. 3, pp 277–278. (b) Verkade, J. G. *Phosphorus Sulfur* **1976**, *2*, 251.
18. Gilheany, D. G. *Chem. Rev.* **1994**, *94*, 1339.
19. Dobado, J. A.; Martínez-García, H.; Molina-Molina, J.; Sondberg, M. R. *J. Am. Chem. Soc.* **1998**, *120*, 8461.
20. Majoral, J.-P.; Pujol, R.; Navech, J. *Bull. Soc. Chim. Fr.* **1972**, 606.
21. Gagnaire, D.; Robert, J. B. *Bull. Soc. Chim. Fr.* **1967**, 2240.
22. Bartle, K. D.; Edmundson, R. S.; Jones, D. W. *Tetrahedron* **1967**, *23*, 1701.
23. Katritzky, A. R.; Nesbit, M. R.; Michalski, J.; Tulmowski, Z.; Zwierzak, A. *J. Chem. Soc. (B)* **1970**, 140.
24. Eliel, E. L. *Chem. Ind. (Lond.)* **1959**, 568.
25. It is noteworthy that McKenna has questioned the veracity of Eq. (1) because of the use of anchoring groups in the anancomeric models, which might distort the geometry of the ring McKenna, J. *Tetrahedron* **1974**, *30*, 1555.
26. Edmundson, R. S.; Mitchell, E. W. *J. Chem. Soc. (C)* **1970**, 752.
27. Harris, R. K.; Katritzky, A. R.; Musierowics, S.; Ternai, B. *J. Chem. Soc. (A)* **1967**, 37.
28. Majoral, J.-P.; Bergounhou, C.; Navech, J. *Bull. Soc. Chim. Fr.* **1973**, 3146.
29. Setzer, W. N.; Sopchik, A. E.; Bentrude, W. G. *J. Am. Chem. Soc.* **1985**, *107*, 2083.

30. Bajwa, G. S.; Bentrude, W. G.; Pantaleo, N. S.; Newton, M. G.; Hargis, J. H. *J. Am. Chem. Soc.* **1979**, *101*, 1602.
31. Eliel, E. L.; Wilen, S. H.; Mander, L. N. *Stereochemistry of Organic Compounds*; Wiley: New York, 1994; chapter 11.
32. Klyne, W.; Prelog, V. *Experientia* **1972**, *16*, 521.
33. Brock, C. P.; Dunitz, J. D. *Chem. Mater.* **1994**, *6*, 1118.
34. Stout, G. H.; Jensen, L. H. *X-Ray Structure Determination. A Practical Guide*; 2nd ed; Wiley: New York, 1989; Part III.
35. Eliel, E. L.; Gordillo, B.; White, P. S.; Harris, D. L. *Heteroatom. Chem.* **1997**, *8*, 509.
36. Romers, C.; Altona, C.; Havinga, E. *Top. Stereochem.* **1969**, *4*, 39.
37. Hutchins, R. O.; Maryanoff, B. E.; Castillo, M. J.; Hargrave, K. D.; McPhail, A. T. *J. Am. Chem. Soc.* **1979**, *101*, 1600.
38. Kinas, R.; Stec, W. J.; Krüger, C. *Phosphorus Sulfur* **1978**, *4*, 295.
39. (a) Drew, M. G. B.; Rodgers, J. *Acta Crystallogr.* **1972**, *B28*, 924. (b) Drew, M. G. B.; Rodgers, J.; White, D. W.; Verkade, J. G. *J. Chem. Soc. Chem. Commun.* **1971**, 227.
40. Sim, G. A. *Acta Crystallogr.* **1990**, *B46*, 676.
41. Hommer, H.; Domínguez, Z.; Gordillo, B. *Acta Crystallogr.* **1998**, *C54*, 832.
42. Bondi, A. J. *Phys. Chem.* **1964**, *68*, 441.
43. Tokiwa, H.; Ichikawa, H. *Int. J. Quant. Chem.* **1994**, *50*, 109.
44. Enraf-Nonius. CAD-4 Software. Version 5.0, Enraf-Nonius, Delft: The Netherlands, 1989.
45. Petricek, V., Dusek, M. JANA98, Institute of Physics, Academy of Sciences of Czech Republic Praha.
46. Sheldrick, G. M. *Acta Crystallogr.* **1990**, *A46*, 467.
47. Sheldrick, G. M. SHELXL93. Program for the Refinement of Crystal Structures, University of Göttingen, Germany.
48. Sheldrick, G. M. SHELXL97. Program for the Refinement of Crystal Structures, University of Göttingen, Germany.
49. Zsolnai, L. A Graphical Molecular Program, University of Heildelberg, Denmark.
50. (a) Nardelli, M. *Computer Chem.* **1983**, *7*, 95. (b) Nardelli, M. *J. Appl. Crystallogr.* **1995**, *28*, 659.
51. Gordillo, B.; Hernández, J. *Org. Prep. Proc. Int.* **1997**, *29*, 195.